



**QUEEN'S
UNIVERSITY
BELFAST**

An investigation of Fe XVI emission lines in solar and stellar extreme-ultraviolet and soft X-ray spectra

Keenan, F. P., Drake, J. J., & Aggarwal, K. M. (2007). An investigation of Fe XVI emission lines in solar and stellar extreme-ultraviolet and soft X-ray spectra. *Monthly Notices of the Royal Astronomical Society*, 381, 1727-1732. <https://doi.org/10.1111/j.1365-2966.2007.12365.x>

Published in:
Monthly Notices of the Royal Astronomical Society

Document Version:
Publisher's PDF, also known as Version of record

Queen's University Belfast - Research Portal:
[Link to publication record in Queen's University Belfast Research Portal](#)

Publisher rights

© 2007 The Authors

This article has been accepted for publication in *Monthly Notices of the Royal Astronomical Society* ©: 2007. Published by Oxford University Press on behalf of the Royal Astronomical Society. All rights reserved.

General rights

Copyright for the publications made accessible via the Queen's University Belfast Research Portal is retained by the author(s) and / or other copyright owners and it is a condition of accessing these publications that users recognise and abide by the legal requirements associated with these rights.

Take down policy

The Research Portal is Queen's institutional repository that provides access to Queen's research output. Every effort has been made to ensure that content in the Research Portal does not infringe any person's rights, or applicable UK laws. If you discover content in the Research Portal that you believe breaches copyright or violates any law, please contact openaccess@qub.ac.uk.

An investigation of Fe xvi emission lines in solar and stellar extreme-ultraviolet and soft X-ray spectra

F. P. Keenan,^{1*} J. J. Drake² and K. M. Aggarwal¹

¹*Astrophysics Research Centre, School of Mathematics and Physics, Queen's University, Belfast BT7 1NN*

²*Smithsonian Astrophysical Observatory, MS 3, 60 Garden Street, Cambridge, MA 02138, USA*

Accepted 2007 August 15. Received 2007 June 29

ABSTRACT

New fully relativistic calculations of radiative rates and electron impact excitation cross-sections for Fe xvi are used to determine theoretical emission-line ratios applicable to the 251–361 and 32–77 Å portions of the extreme-ultraviolet (EUV) and soft X-ray spectral regions, respectively. A comparison of the EUV results with observations from the Solar Extreme-Ultraviolet Research Telescope and Spectrograph (SERTS) reveals excellent agreement between theory and experiment. However, for emission lines in the 32–49 Å portion of the soft X-ray spectral region, there are large discrepancies between theory and measurement for both a solar flare spectrum obtained with the X-Ray Spectrometer/Spectrograph Telescope (XSST) and for observations of Capella from the Low-Energy Transmission Grating Spectrometer (LETGS) on the *Chandra X-ray Observatory*. These are probably due to blending in the solar flare and Capella data from both first-order lines and from shorter wavelength transitions detected in second and third order. By contrast, there is very good agreement between our theoretical results and the XSST and LETGS observations in the 50–77 Å wavelength range, contrary to previous results. In particular, there is no evidence that the Fe xvi emission from the XSST flare arises from plasma at a much higher temperature than that expected for Fe xvi in ionization equilibrium, as suggested by earlier work.

Key words: atomic data – Sun: activity – Sun: corona – Sun: X-rays, gamma-rays.

1 INTRODUCTION

Emission lines arising from transitions in ions of the sodium isoelectronic sequence are widely detected in solar ultraviolet, extreme-ultraviolet (EUV) and soft X-ray spectra (see e.g. Acton et al. 1985; Sandlin et al. 1986; Thomas & Neupert 1994). It has long been known that these lines provide electron temperature diagnostics for coronal plasmas (Flower & Nussbaumer 1975), electron density estimates for laboratory sources (Feldman & Doschek 1977), and allow the determination of element abundances (Laming & Feldman 1999). However, to reliably model these emission features requires highly accurate atomic data, especially for electron impact excitation rates (Mason & Monsignori Fossi 1994).

The most frequently observed Na-like ion in the Sun is Fe xvi, which is not surprising due to the large Fe cosmic abundance. This ion provides some of the strongest solar emission features at both EUV and soft X-ray wavelengths, which have been the topic of several papers. The most recent examples include the work of Keenan et al. (2003) on EUV observations from the Solar Extreme-Ultraviolet Research Telescope and Spectrograph (SERTS), mod-

elled using electron impact excitation rates calculated with the R-matrix code by Eissner et al. (1999). In the soft X-ray spectral region, Cornille et al. (1997) analysed a solar flare spectrum with excitation rates determined by these authors in the distorted-wave approximation.

However, the atomic physics calculations of Eissner et al. (1999) and Cornille et al. (1997) for Fe xvi only considered transitions among the $n \leq 4$ and $n \leq 5$ levels, respectively. More recently, Aggarwal & Keenan (2006) have generated excitation rates for Fe xvi using the fully relativistic Dirac R-matrix code, which include several improvements over previous calculations, and in particular the inclusion of all levels with $n \leq 7$. In this paper, we use the Aggarwal & Keenan data to derive theoretical emission-line strengths for Fe xvi and compare these with both solar and stellar EUV and soft X-ray observations.

2 ATOMIC DATA AND THEORETICAL LINE RATIOS

The model ion adopted for Fe xvi consisted of the 39 energetically lowest fine-structure levels arising from the $n \leq 7$ ($\ell \leq 4$) configurations. Energies for all these levels were obtained from the experimental compilation in the National Institute of Standards and

*E-mail: F.Keenan@qub.ac.uk

Technology (NIST) data base¹ where available. However, in the case of the $6\text{ g }^2\text{G}_{7/2,9/2}$ and $7\text{ g }^2\text{G}_{7/2,9/2}$ levels, energies were taken from the theoretical results of Aggarwal & Keenan (2006). Test calculations including higher lying levels were found to have a negligible effect on the theoretical line ratios considered in this paper.

Electron impact excitation rates for transitions among the levels discussed above were obtained from Aggarwal & Keenan (2006), as were Einstein A coefficients for allowed and forbidden transitions. However, we note that the allowed emission lines of Fe xvi considered here will be in the coronal approximation (Elwert 1952), unless the electron density (N_e) is greater than 10^{16} cm^{-3} (Feldman & Doschek 1977), much higher than found in solar or stellar coronae. Hence, the line intensities (and ratios) will depend primarily on the excitation rates from the ground state, and will not be sensitive to the adopted A values.

As has been discussed by, for example, Seaton (1964), proton excitation may sometimes be important for transitions with small excitation energies, that is, fine-structure transitions. However, test calculations for Fe xvi setting the proton rates for $^2\text{P}_{1/2}-^2\text{P}_{3/2}$, $^2\text{D}_{3/2}-^2\text{D}_{5/2}$, $^2\text{F}_{5/2}-^2\text{F}_{7/2}$ and $^2\text{G}_{7/2}-^2\text{G}_{9/2}$ to even 100 times larger than the corresponding electron excitation rates had a negligible effect on the level populations, showing this atomic process to be unimportant, at least under solar conditions.

Using the atomic data discussed above in conjunction with a recently updated version of the statistical equilibrium code of Dufton (1977), relative Fe xvi level populations, and hence emission-line strengths were calculated for a range of electron temperatures ($T_e = 10^{6.1}-10^{7.1}\text{ K}$ in steps of 0.1 dex), over which Fe xvi has a fractional abundance in ionization equilibrium of $N(\text{Fe xvi})/N(\text{Fe}) \geq 3 \times 10^{-4}$ (Mazzotta et al. 1998). The following assumptions were made in the calculations: (i) that ionization to and recombination from other ionic levels are slow compared with bound-bound rates, (ii) that photoexcitation and induced de-excitation rates are negligible in comparison with the corresponding collision rates and (iii) that all transitions are optically thin.

Our results are far too extensive to reproduce here, as with 39 fine-structure levels in our calculations we have intensities for 741 transitions at each of the 11 values of T_e . However, results involving any line pair, in either photon or energy units, are freely available from one of the authors (FPK) by email on request. Given expected errors in the adopted atomic data of at worst ± 20 per cent (see Aggarwal & Keenan 2006), we would expect our line ratio calculations to be accurate to better than ± 30 per cent.

3 OBSERVATIONAL DATA

We compare our Fe xvi line ratio calculations with several data sets. For EUV transitions, we employ observations of several solar features obtained with the rocket-borne SERTS spectrograph, while for soft X-ray lines, we utilize a solar flare spectrum also taken with rocket-borne instrument, plus a composite spectrum of Capella from the *Chandra X-ray Observatory*. These data sets are discussed separately below.

3.1 Solar EUV observations

Keenan et al. (2003) have summarized line intensity ratio measurements involving the Fe xvi EUV transitions between 251 and 361 Å, determined from solar spectra of several quiet and active regions,

Table 1. Fe xvi transitions in SERTS spectra.

Wavelength (Å)	Transition
251.07	$3\text{p}^2\text{P}_{1/2}-3\text{d}^2\text{D}_{3/2}$
262.98	$3\text{p}^2\text{P}_{3/2}-3\text{d}^2\text{D}_{5/2}$
265.02	$3\text{p}^2\text{P}_{3/2}-3\text{d}^2\text{D}_{3/2}$
335.40	$3\text{s}^2\text{S}_{1/2}-3\text{p}^2\text{P}_{3/2}$
360.75	$3\text{s}^2\text{S}_{1/2}-3\text{p}^2\text{P}_{1/2}$

Table 2. Comparison of theoretical Fe xvi emission-line intensity ratios with average values from SERTS.

Line ratio	Observed	Present theory ^a	CHIANTI theory ^a
335.40/360.75	2.2 ± 0.2	2.1	2.1
251.07/335.40	0.049 ± 0.008	0.049	0.044
262.98/335.40	0.066 ± 0.012	0.081	0.074
265.02/335.40	0.0085 ± 0.0015	0.0078	0.0071

^aPresent theoretical ratios and those from CHIANTI calculated in energy units at $T_e = 10^{6.4}\text{ K}$ and $N_e = 10^{10}\text{ cm}^{-3}$.

a small subflare and an off-limb area, obtained with the SERTS instrument. The SERTS data sets have spectral resolutions of typically 50–80 mÅ (full width at half-maximum) in first order, and probably provide the best observations for investigating EUV lines of Fe xvi. For example, the *Skylab* S082A spectra analysed by Keenan et al. (1994) had a spectral resolution of only about 200 mÅ, and the stronger Fe xvi emission features were often saturated on the photographic film used to record the data. The SERTS observations are of higher spectral resolution and show at worst only a slight indication of saturation, which does not significantly affect the measured line intensities (Thomas & Neupert 1994). They have therefore been adopted in the present analysis. Further information on the SERTS observations, including details of the wavelength and absolute flux calibration procedures employed in their reduction, may be found in Thomas & Neupert and Brosius et al. (1996) and Brosius, Davila & Thomas (1998).

In Table 1, we list the Fe xvi transitions detected in the SERTS spectra, along with their experimental wavelengths (Thomas & Neupert 1994), while Table 2 shows the averages of the line ratio values measured by Keenan et al. (2003). We analyse the averages rather than the individual ratios for each solar feature detected by SERTS, as the Fe xvi emission-line intensities are predicted to be N_e -insensitive (see Section 2), and could reasonably be expected to all be formed at the same temperature (that of maximum fractional abundance in ionization equilibrium). Therefore, the ratio values should be independent of the solar feature observed. By considering the average ratios, we can reduce the experimental error bars and hence improve the comparison with theory.

3.2 Solar flare soft X-ray observations

The most detailed measurements to date of Fe xvi soft X-ray emission lines remain those made by the X-ray Spectrometer/Spectrograph Telescope (XSST) during a rocket flight on 1982 July 13 (Acton et al. 1985). This instrument recorded the spectrum of an M class flare on Kodak 101–07 emulsion, spanning the wavelength range 11–97 Å at a spectral resolution of 0.02 Å. The XSST made two exposures, one of 54 s and the other of 145 s, and the

¹ <http://physics.nist.gov/PhysRefData/>.

Table 3. Fe XIII transitions in the XST solar flare and *Chandra* LETGS Capella spectra.

Wavelength (Å)	Transition	Note
32.66	$3p^2P_{3/2}-7d^2D_{3/2,5/2}$	Blend with Ca XII ^a ; blend with Fe XVII and Fe XIX in second order ^b
34.86	$3p^2P_{1/2}-6d^2D_{3/2}$	Possible blend with C V, S XII and Ar XII ^b
35.10	$3p^2P_{3/2}-6d^2D_{3/2,5/2}$	Possible blend with Fe XXII and Fe XXIII in third order ^b
35.73	$3p^2P_{1/2}-6s^2S_{1/2}$	Blend with Ca XI ^b
36.01	$3p^2P_{3/2}-6s^2S_{1/2}$	Blend with unidentified feature on blue wing ^b
36.75	$3s^2S_{1/2}-5p^2P_{3/2}$	Blend with Fe XVII in third order ^b
36.80	$3s^2S_{1/2}-5p^2P_{1/2}$	Blend with Fe XVII in third order ^b
39.83	$3p^2P_{1/2}-5d^2D_{3/2}$	
40.14	$3p^2P_{3/2}-5d^2D_{3/2,5/2}$	
40.19	$3d^2D_{3/2}-6f^2F_{5/2}$	Blend with wing of C V ^b
40.27	$3d^2D_{5/2}-6f^2F_{5/2,7/2}$	Blend with C V ^{a,b}
41.90	$3p^2P_{1/2}-5s^2S_{1/2}$	Blend with Fe XV ^a ; possible blend with Fe XVIII and Fe XXI in third order ^b
42.27	$3p^2P_{3/2}-5s^2S_{1/2}$	Blend with Fe XX and Ni XIX in third order ^b
46.66	$3d^2D_{3/2}-5f^2F_{5/2}$	Blend with wing of 46.72 Å feature ^b
46.72	$3d^2D_{5/2}-5f^2F_{5/2,7/2}$	Blend with wing of 46.66 Å feature ^b
48.97	$3d^2D_{5/2}-5p^2P_{3/2} + 3d^2D_{3/2}-5p^2P_{1/2}$	Blend with Fe XVII in third order ^b
50.35	$3s^2S_{1/2}-4p^2P_{3/2}$	Blend with Fe XVII in third order ^b
50.56	$3s^2S_{1/2}-4p^2P_{1/2}$	Blend with Si X ^b
54.13	$3p^2P_{1/2}-4d^2D_{3/2}$	
54.72	$3p^2P_{3/2}-4d^2D_{5/2}$	
54.77	$3p^2P_{3/2}-4d^2D_{3/2}$	
62.88	$3p^2P_{1/2}-4s^2S_{1/2}$	
63.72	$3p^2P_{3/2}-4s^2S_{1/2}$	
66.25	$3d^2D_{3/2}-4f^2F_{5/2}$	
66.36	$3d^2D_{5/2}-4f^2F_{5/2,7/2}$	Blend with O VII in third order ^b
74.36	$4p^2P_{1/2}-7s^2S_{1/2}$	Blend with N VII in third order ^b
76.50	$3d^2D_{5/2}-4p^2P_{3/2}$	Possible blend with Fe X ^b
76.80	$3d^2D_{3/2}-4p^2P_{1/2}$	Possible blend with Fe X ^b

^aFrom Acton et al. (1985) paper on the XST solar flare spectrum.^bFrom this work on the Capella spectrum.

observations presented by Acton et al. are for the latter. Further details of the XST instrument may be found in Brown et al. (1979) and Bruner et al. (1980), while the reduction and calibration of the observations are discussed in Acton et al.

In Table 3, we list the Fe XVI transitions identified in the XST spectrum by Acton et al. (1985), along with their measured wavelengths. We also indicate possible blending lines or alternative identifications, as suggested by Acton et al. Additionally, we have used line lists, such as the NIST data base and the Atomic Line List of Peter van Hoof² to investigate if any other emission features in the Acton et al. data set may be due to Fe XVI. However, only one possible identification was forthcoming, namely an emission feature at 74.36 Å which is coincident with a predicted Fe XVI transition.

The intensity of the 54.72 Å line of Fe XVI measured by Acton et al. (1985) in the XST spectrum is given in Table 4; observed intensities of the other Fe XVI transitions may be inferred from this using the line ratio values provided in the table. Brown et al. (1986) note that the relative intensities of lines in the XST spectrum similar in strength to the Fe XVI transitions discussed here should be accurate to about ± 20 per cent, and hence line ratios to ± 30 per cent. Evidence for this comes from, for example, our previous analyses of Ni XVIII and Fe XV emission lines in the XST observations (Keenan et al. 1999, 2006). We found that, for line ratios involving unblended transitions, agreement between theory and observation was excellent, with differences that average only 11 per cent for

Ni XVIII and 20 per cent for Fe XV. The observed XST Fe XVI line ratios in Table 4 have therefore been assigned a uniform ± 30 per cent uncertainty.

3.3 Capella spectrum

The Capella observations analysed here are described in detail by Keenan et al. (2006). Spectra were co-added from six separate observations obtained by the Low-Energy Transmission Grating Spectrograph (LETGS) on the *Chandra X-ray Observatory*, employing the High-Resolution Camera spectroscopic detector (HRC-S) in its standard configuration, yielding a resolution of approximately 0.06 Å (see e.g. Weisskopf et al. 2003, for further details).

The analysis of the co-added Capella spectrum followed methods described by Keenan et al. (2006), to which the reader is referred for further details, and employed the PINTOFAL³ IDL⁴ software suite (Kashyap & Drake 2000). Line fluxes were measured by fitting ‘modified Lorentzian’, or Moffat, functions of the form $F(\lambda) = a/(1 + (\frac{\lambda - \lambda_0}{\Gamma})^\beta)$, where a is the amplitude, Γ is a characteristic line width and $\beta = 2.4$ (Drake 2004). As in our earlier work, line positions were allowed to vary from their predicted wavelengths by ≤ 0.05 Å, this being dictated by imaging distortions in the detector (see e.g. Chung et al. 2004). For lines closely spaced in wavelength,

² <http://www.pa.uky.edu/~peter/atomic/>.³ Available from <http://hea-www.harvard.edu/PINTofALE/>.⁴ Interactive Data Language, Research Systems Inc.

Table 4. Comparison of theoretical Fe xvi emission-line intensity ratios with XST solar flare and Capella observations.

Line ratio	Observed XST ^a	Observed Capella ^b	Present theory ^c	CHIANTI theory ^c
32.66/54.72	0.38 ± 0.11	0.08 ± 0.03	0.023	–
34.86/54.72	0.099 ± 0.030	0.09 ± 0.04	0.027	–
35.10/54.72	0.17 ± 0.05	0.16 ± 0.04	0.055	–
35.73/54.72	0.049 ± 0.015	0.05 ± 0.04	0.017	–
36.01/54.72	0.049 ± 0.015	0.11 ± 0.04	0.035	–
36.75/54.72	0.22 ± 0.07	0.22 ± 0.04	0.089	0.094
36.80/54.72	0.22 ± 0.07	0.31 ± 0.04	0.045	0.051
39.83/54.72	0.35 ± 0.11	0.12 ± 0.06	0.088	0.12
40.14/54.72	0.55 ± 0.17	0.33 ± 0.07	0.18	0.24
40.19/54.72	0.14 ± 0.04	0.04 ± 0.04	0.030	–
40.27/54.72	0.59 ± 0.18	0.93 ± 0.09	0.045	–
41.90/54.72	0.14 ± 0.04	0.22 ± 0.21	0.077	0.16
42.27/54.72	0.14 ± 0.04	0.35 ± 0.13	0.16	0.33
46.66/54.72	0.27 ± 0.08	0.28 ± 0.02	0.12	0.15
46.72/54.72	0.37 ± 0.11	0.28 ± 0.03	0.17	0.23
48.97/54.72	0.099 ± 0.030	0.06 ± 0.02	0.034	0.035
50.35/54.72	0.87 ± 0.26	1.35 ± 0.04	0.72	0.51
50.56/54.72	0.44 ± 0.13	0.47 ± 0.03	0.38	0.28
54.13/54.72	0.70 ± 0.21	0.68 ± 0.05	0.55	0.56
54.77/54.72	0.16 ± 0.05	0.07 ± 0.05	0.11	0.11
62.88/54.72	0.88 ± 0.26	0.62 ± 0.07	1.1	1.6
63.72/54.72	1.6 ± 0.5	1.18 ± 0.07	2.2	3.4
66.25/54.72	0.99 ± 0.30	0.73 ± 0.05	1.0	1.1
66.36/54.72	1.3 ± 0.4	1.13 ± 0.05	1.6	1.7
74.36/54.72	0.12 ± 0.04	–	0.0042	–
76.50/54.72	0.36 ± 0.11	0.28 ± 0.04	0.26	0.17
76.80/54.72	0.15 ± 0.05	0.11 ± 0.05	0.15	0.10

^a $I(54.72 \text{ \AA}) = 223 \pm 45 \text{ photons cm}^{-2} \text{ s}^{-1} \text{ arcsec}^{-2}$.^b $I(54.72 \text{ \AA}) = (3.89 \pm 0.17) \times 10^{-5} \text{ photons cm}^{-2} \text{ s}^{-1}$.^cPresent theoretical ratios and those from CHIANTI calculated in photon units at $T_e = 10^{6.4} \text{ K}$ and $N_e = 10^{10} \text{ cm}^{-3}$.

their relative separations were kept fixed to their reference values, while the position of the group was allowed to vary.

As found in our earlier study (Keenan et al. 2006), lines from the $n = 2$ shell of abundant elements such as Mg, Si, S and Ar plus the $n = 3$ shell of Fe, together with strong features from shorter wavelength transitions arising from higher spectral orders, are also frequently detected in the 30–80 Å range. Unlike the *Chandra* ACIS CCD detector, the HRC-S microchannel plate detector possesses no energy resolution of its own and overlapping spectral orders cannot be separated. Prior to performing line fits, we therefore searched for the presence of significant blends from known strong lines in first and higher orders. This was undertaken by computing the strengths of lines in the latest version (version 5.2) of the CHIANTI data base (Dere et al. 1997; Landi et al. 2006) within our wavelength range of interest using the differential emission measure (DEM) distribution of Raassen & Kaastra (2007). Relevant blends are noted in Table 3.

As with the XST observations (Section 3.2), the measured intensity of the 54.72 Å line is given in Table 4, and those of the other Fe xvi transitions may be inferred from this using the line ratio values. It should be kept in mind in the interpretation of the measured fluxes that they are also prone to uncertainty caused by hidden blends of unidentified lines. For such cases, there is an expectation that the measured fluxes might be systematically too high. Since the resolving power of the *Chandra* LETGS is a factor of approximately 3 lower than that of the XST, blends tend to be more of a problem. We discuss this further in Section 4.

4 RESULTS AND DISCUSSION

In Table 2, we list the average observed Fe xvi EUV emission-line ratios from the SERTS data sets, along with the theoretical results at the electron temperature of maximum fractional abundance for Fe xvi in ionization equilibrium, $T_e = 10^{6.4} \text{ K}$ (Mazzotta et al. 1998). Also given in the table are the calculated ratios from the CHIANTI data base, which employs the radiative rates and electron impact excitation cross-sections of Sampson, Zhang & Fontes (1990). The Sampson et al. excitation cross-section results are in very good agreement (generally better than 10 per cent) with those of Cornille et al. (1997), except for $3s^2S_{1/2} - 5s^2S_{1/2}$, where there is a difference of 25 per cent at low energies. An inspection of Table 2 reveals excellent agreement between observation and theory for all of the line ratios. In some instances there are smaller discrepancies with the present calculations than with those from CHIANTI and vice versa. However, both sets of theoretical results clearly agree with experiment once the observational uncertainties are taken into account.

In Table 4, we similarly list the observed Fe xvi soft X-ray emission-line ratios from the XST solar flare and Capella spectra, along with the present calculations and those from CHIANTI at $T_e = 10^{6.4} \text{ K}$. We note that the temperature of formation of the Fe xvi lines studied here is increased to $T_e \approx 10^{6.7} \text{ K}$, when weighted by the Capella DEM, and hence theoretical line ratios at this higher value of T_e should be employed for comparison with the Capella observations. However, for the line ratios in Table 4, the theoretical values at $T_e = 10^{6.4} \text{ K}$ differ, on average, by only 12 per cent from those at $T_e = 10^{6.7} \text{ K}$. For ratios involving transitions in the wavelength range 41.90–76.80 Å, the discrepancies are even smaller, averaging only 7 per cent. As a consequence, changing the theoretical ratios in Table 4 to values for $T_e = 10^{6.7} \text{ K}$ would not alter the discussion below. For example, the theoretical intensity ratio $I(32.66 \text{ \AA})/I(54.72 \text{ \AA})$ in Table 4 is 0.023, while the value at $T_e = 10^{6.7} \text{ K}$ is 0.032, still much smaller than the XST and Capella measurements of 0.38 and 0.08, respectively.

The CHIANTI results in Table 4 are not available for all transitions due to the limited model ion considered by this data base, which only incorporates levels up to and including $5f^2F_{5/2,7/2}$. As noted in Section 3.2, the 54.72 Å transition has been used as the denominator for all of the Fe xvi line ratios, as it is one of the strongest Fe xvi emission features in the XST and Capella spectral ranges, and hence should be free from blends. To confirm this, we have generated synthetic flare and Capella spectra using CHIANTI, which reveal no nearby emission lines which will contribute more than 3 per cent to the 54.72 Å intensity.

An inspection of Table 4 and Fig. 1 (where we plot observed/theoretical Fe xvi line ratios as a function of wavelength) reveals generally very poor agreement between theory and observation for line ratios involving Fe xvi transitions with wavelengths $\leq 48.97 \text{ \AA}$, for both the solar and Capella spectra. In the majority of instances, the measured ratios are larger than the theoretical values both from the present calculations and from CHIANTI. These differences are too large to be explained by possible errors in the adopted electron temperature, as the line ratios are not that sensitive to T_e . For example, changing T_e from $10^{6.4} \text{ K}$ to even as large a value as $T_e = 10^{6.9} \text{ K}$ only leads to the theoretical intensity ratio $I(34.86 \text{ \AA})/I(54.72 \text{ \AA})$ increasing from 0.027 to 0.038, still much lower than the measurements of 0.099 and 0.09 for the Sun and Capella, respectively. Similarly, $I(36.80 \text{ \AA})/I(54.72 \text{ \AA})$ increases from 0.045 to 0.067, compared to the experimental ratios of 0.22 for the Sun and 0.31 for Capella.

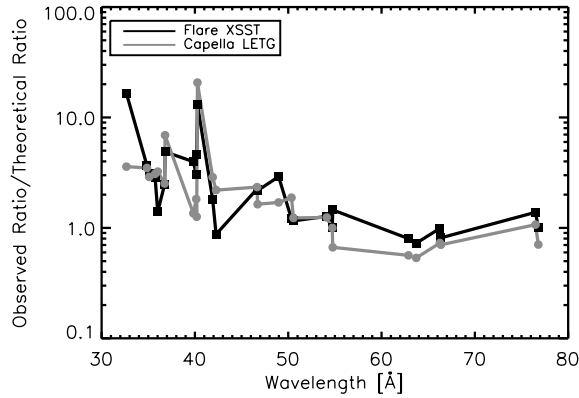


Figure 1. Comparison of observed and predicted ratios of Fe XVI line intensities, $I(\lambda)/I(54.72 \text{ Å})$, for the XSST spectrum of a solar flare and *Chandra* observations of Capella, plotted as a function of numerator line wavelength.

One possible cause for the discrepancies is an error in the instrument intensity calibrations. Some support for this comes from discrepancies in several of the Fe XVI lines when ratioed against 54.72 Å , but not when compared with each other. For example, the observed values of $I(34.86 \text{ Å})/I(54.72 \text{ Å})$ and $I(35.10 \text{ Å})/I(54.72 \text{ Å})$ are much larger than theory, but the measured $I(34.86 \text{ Å})/I(35.10 \text{ Å})$ ratios are 0.58 and 0.56 for the XSST and Capella spectra, respectively, in good agreement with the theoretical prediction of 0.49. On the other hand, $I(36.75 \text{ Å})/I(36.80 \text{ Å})$ involves two lines very close together in wavelength, yet is predicted to be 2.0 and has measured values of only 1.0 for the solar flare and 0.71 for Capella. Moreover, the *Chandra* LETGS calibration is thought to be accurate to approximately 15 per cent in absolute terms across most of its band, with relative calibration uncertainties over narrow wavelength intervals being significantly smaller. It is therefore unlikely the larger discrepancies between theory and observation for Capella can be explained by calibration errors.

An alternative explanation for the discrepancies is blending of the Fe XVI emission features, with instances of good agreement such as $I(34.86 \text{ Å})/I(35.10 \text{ Å})$ being simply due to coincidence. We believe this to be the much more likely alternative, as the CHIANTI synthetic solar flare and Capella spectra indicate that most of the Fe XVI lines in the 32–49 Å wavelength range are blended with lines of highly ionized Fe and other ions, such as Fe XVII and Fe XXII, appearing in the observations in second or third order (see Table 3). Furthermore, Acton et al. (1985) note a strong second-order spectrum falling between 25 and 50 Å in the XSST data set. In the case of Capella, second order is suppressed to some extent by the 1:1 grating bar width-to-spacing ratio, and third order is most prominent. Additionally, it is interesting to note that for the few Fe XVI transitions in this wavelength range which the CHIANTI synthetic spectra indicate are not too blended (at least in the XSST observations), such as 36.01 and 42.27 Å, agreement between theory and observation is good.

For Fe XVI transitions with wavelengths $\geq 50.35 \text{ Å}$, an inspection of Table 4 and Fig. 1 reveals that agreement between the present theoretical line ratio calculations and the observations is very good for both the solar and Capella spectra, with the exception of $I(74.36 \text{ Å})/I(54.72 \text{ Å})$. Our calculations indicate that the 74.36 Å line is not due to Fe XVI, with the CHIANTI synthetic flare spectrum suggesting an alternative identification of Ne IX $1s2s^3S_1-1s3p^3P_2$, as the predicted intensity ratio of this feature to that of Fe XV 73.47 Å ,

$I(74.36 \text{ Å})/I(73.47 \text{ Å}) = 0.41$, is in reasonable agreement with the measured value of $I(74.36 \text{ Å})/I(73.47 \text{ Å}) = 0.22 \pm 0.07$.

For the other line ratios spanning 50.35–76.80 Å, the discrepancies between the measurements and the current calculations average only 18 per cent for the XSST spectrum and 30 per cent for the Capella observations. For the latter, the average discrepancy is reduced to 27 per cent if we compare the measurements with the theoretical ratios generated at the electron temperature appropriate to the Fe XVI emission from Capella, that is, $T_e = 10^{6.7} \text{ K}$. By contrast, there are large differences between experiment and the CHIANTI theoretical results, of more than a factor of 2 in the case of $I(63.72 \text{ Å})/I(54.72 \text{ Å})$. The calculations of Cornille et al. (1997) show similar discrepancies with the XSST measurements, as these authors adopted similar atomic data to those employed in CHIANTI (see Section 2). Cornille et al. suggested that the Fe XVI emission in the XSST flare was at an electron temperature above $10^{6.7} \text{ K}$, as such a high value of T_e was required to provide agreement between the theoretical and observed line ratios. However, the present results show that there is no need to invoke a very high temperature for the XSST flare, with ratios calculated at the temperature of Fe XVI maximum abundance in ionization equilibrium ($T_e = 10^{6.4} \text{ K}$) being consistent with the observations.

5 CONCLUSIONS

Theoretical Fe XVI EUV and soft X-ray line intensity ratios based on new fully-relativistic calculations of radiative rates and electron impact excitation cross-sections have been compared with measurements from spectra of the Sun and the binary star Capella. Line intensity ratios obtained from SERTS EUV observations are in excellent agreement with the new theoretical values. In the soft X-ray regime, lines shortwards of 50 Å in both solar flare and Capella spectra are found to be too blended by first- and higher-order transitions, particularly from high-ionization stages of Fe, to provide useful comparisons with the theoretical ratios. However, the measured intensity ratios $I(\lambda)/I(54.72 \text{ Å})$ for lines with $\lambda > 50 \text{ Å}$ are in good agreement with the new theoretical results, with mean discrepancies of 18 and 27 per cent for the flare and Capella observations, respectively. This represents a considerable improvement over earlier theoretical predictions of the Fe XVI spectrum.

ACKNOWLEDGMENTS

KMA acknowledges financial support from EPSRC, while FPK is grateful to AWE Aldermaston for the award of a William Penney Fellowship. The authors thank Peter van Hoof for the use of his Atomic Line List. CHIANTI is a collaborative project involving the Naval Research Laboratory (USA), Rutherford Appleton Laboratory (UK), Mullard Space Science Laboratory (UK), and the Universities of Florence (Italy) and Cambridge (UK) and George Mason University (USA).

REFERENCES

- Acton L. W., Bruner M. E., Brown W. A., Fawcett B. C., Schweizer W., Speer R. J., 1985, *ApJ*, 291, 865
- Aggarwal K. M., Keenan F. P., 2006, *A&A*, 450, 1249
- Brosius J. W., Davila J. M., Thomas R. J., Monsignori-Fossi B. C., 1996, *ApJS*, 106, 143
- Brosius J. W., Davila J. M., Thomas R. J., 1998, *ApJS*, 119, 255

- Brown W. A., Bruner E. C., Acton L. W., Franks A., Stedman M., Speer R. J., 1979, in Weisskopf M. C., ed., Proc. SPIE Vol. 184, Space Optics Imaging X-ray Optics Worldshop. SPIE, Bellingham WA, p. 278
- Brown W. A., Bruner M. E., Acton L. W., Mason H. E., 1986, ApJ, 301, 981
- Bruner E. C., Brown W. A., Salat S. W., Franks A., Schmidtke G., Schweizer W., Speer R. J., 1980, Opt. Eng., 19, 433
- Chung S. M., Drake J. J., Kashyap V. L., Ratzlaff P. W., Wargelin B. J., 2004, in Hasinger G., Turner M. J. L., eds, Proc. SPIE Vol. 5488, UV and Gamma-Ray Space Telescope Systems. SPIE, Bellingham WA, p. 51
- Cornille M., Dubau J., Mason H. E., Blancard C., Brown W. A., 1997, A&A, 320, 333
- Dere K. P., Landi E., Mason H. E., Monsignori-Fossi B. C., Young P. R., 1997, A&AS, 125, 149
- Drake J. J., 2004, Chandra News, 11, 8
- Dufton P. L., 1977, Comput. Phys. Commun., 13, 25
- Eissner W., Galavís M. E., Mendoza C., Zeppen C. J., 1999, A&AS, 136, 385
- Elwert G., 1952, Z. Naturforsch., 7A, 432
- Feldman U., Doschek G. A., 1977, J. Opt. Soc. Am., 67, 726
- Flower D. R., Nussbaumer H., 1975, A&A, 42, 265
- Kashyap V. L., Drake J. J., 2000, Bull. Astron. Soc. India, 28, 475
- Keenan F. P., Conlon E. S., Foster V. J., Tayal S. S., Widing K. G., 1994, ApJ, 432, 809
- Keenan F. P., Mathioudakis M., Pinfield D. J., Brown W. A., Bruner M. E., 1999, Sol. Phys., 185, 289
- Keenan F. P., Katsiyannis A. C., Brosius J. W., Davila J. M., Thomas R. J., 2003, MNRAS, 342, 513
- Keenan F. P., Drake J. J., Chung S., Brickhouse N. S., Aggarwal K. M., Msezane A. Z., Ryans S. I., 2006, ApJ, 645, 597
- Laming J. M., Feldman U., 1999, ApJ, 527, 461
- Landi E., Del Zanna G., Young P. R., Dere K. P., Mason H. E., Landini M., 2006, ApJS, 162, 261
- Mason H. E., Monsignori Fossi B. C., 1994, A&AR, 6, 123
- Mazzotta P., Mazzitelli G., Colafrancesco S., Vittorio N., 1998, A&AS, 133, 403
- Raassen A. J. J., Kaastra J. S., 2007, A&A, 461, 679
- Sampson D. H., Zhang H. L., Fontes C. J., 1990, At. Data Nucl. Data Tables, 44, 209
- Sandlin G. D., Bartoe J.-D. F., Tousey R., Van Hoosier M. E., 1986, ApJS, 61, 801
- Seaton M. J., 1964, MNRAS, 127, 191
- Thomas R. J., Neupert W. M., 1994, ApJS, 91, 461
- Weisskopf M. C. et al., 2003, Exp. Astron., 16, 1

This paper has been typeset from a \TeX/L\AA\TeX file prepared by the author.